ATPase Domain *AFG3L2* Mutations Alter OPA1 Processing and Cause Optic Neuropathy

Leonardo Caporali, ScD, PhD,[1] Stefania Magri, ScD, PhD,[2] Andrea Legati, ScD, PhD,[2] Valentina Del Dotto, ScD, PhD,[3] Francesca Tagliavini, ScD, PhD,[1] Francesca Balistreri, ScD,[2] Alessia Nasca, ScD,[2] Chiara La Morgia, MD, PhD,[1,3] Michele Carbonelli, MD,[1] Maria L. Valentino, MD,[1,3] Eleonora Lamantea, ScD,[2] Silvia Baratta, ScD,[2] Ludger Schöls, MD,[4,5] Rebecca Schüle, MD,[4,5] Piero Barboni, MD,[6,7] Maria L. Cascavilla, MD,[7] Alessandra Maresca, ScD, PhD,[1] Mariantonietta Capristo, ScD, PhD,[1] Anna Ardissone, MD,[8] Davide Pareyson, MD,[9] Gabriella Cammarata, MD,[10] Lisa Melzi, MD,[10] Massimo Zeviani, MD, PhD,[11] Lorenzo Peverelli, MD,[12] Costanza Lamperti, MD, PhD,[2] Stefania B. Marzoli, MD,[10] Mingyan Fang, MD,[13] Matthis Synofzik, MD,[4,5] Daniele Ghezzi, ScD, PhD,[2,14] Valerio Carelli, MD, PhD,[1,3] and Franco Taroni, MD[2]

Objective: Dominant optic atrophy (DOA) is the most common inherited optic neuropathy, with a prevalence of 1:12,000 to 1:25,000. *OPA1* mutations are found in 70% of DOA patients, with a significant number remaining undiagnosed.
Methods: We screened 286 index cases presenting optic atrophy, negative for *OPA1* mutations, by targeted next generation sequencing or whole exome sequencing. Pathogenicity and molecular mechanisms of the identified variants were studied in yeast and patient-derived fibroblasts.
Results: Twelve cases (4%) were found to carry novel variants in *AFG3L2*, a gene that has been associated with autosomal dominant spinocerebellar ataxia 28 (SCA28). Half of cases were familial with a dominant inheritance, whereas the others were sporadic, including *de novo* mutations. Biallelic mutations were found in 3 probands with severe syndromic

View this article online at wileyonlinelibrary.com. DOI: 10.1002/ana.25723

Received Nov 28, 2019, and in revised form Mar 12, 2020. Accepted for publication Mar 20, 2020.

Address correspondence to Dr Taroni, Unit of Medical Genetics and Neurogenetics, Fondazione IRCCS Istituto Neurologico Carlo Besta, via Celoria 11, 20133 Milan, Italy; E-mail: franco.taroni@istituto-besta.it and Dr Carelli, Unit of Neurology, IRCCS Istituto delle Scienze Neurologiche di Bologna, Ospedale Bellaria, Via Altura 1/8, 40139 Bologna, Italy; E-mail: valerio.carelli@unibo.it

L.C., S.M., D.G., V.C., and F.Tar. contributed equally.

From the [1]IRCCS Istituto delle Scienze Neurologiche di Bologna, UOC Clinica Neurologica, Bologna, Italy; [2]Unit of Medical Genetics and Neurogenetics, Fondazione IRCCS Istituto Neurologico Carlo Besta, Milan, Italy; [3]Neurology Unit, Department of Biomedical and Neuromotor Sciences, University of Bologna, Bologna, Italy; [4]Department of Neurodegenerative Diseases, Hertie Institute for Clinical Brain Research and Center of Neurology, University of Tübingen, Tübingen, Germany; [5]German Center for Neurodegenerative Diseases, Tübingen, Germany; [6]Studio Oculistico D'Azeglio, Bologna, Italy; [7]IRCCS Ospedale San Raffaele, Milan, Italy; [8]Unit of Child Neurology, Fondazione IRCCS Istituto Neurologico Carlo Besta, Milan, Italy; [9]Unit of Rare Neurodegenerative and Neurometabolic Diseases, Fondazione IRCCS Istituto Neurologico Carlo Besta, Milan, Italy; [10]Neuro-Ophthalmology Center and Ocular Electrophysiology Laboratory, IRCCS Istituto Auxologico Italiano, Capitanio Hospital, Milan, Italy; [11]Department of Neuroscience, University of Padua, Padua, Italy; [12]Neurology Unit, Azienda Socio Sanitaria Territoriale Lodi, Ospedale Maggiore di Lodi, Lodi, Italy; [13]Beijing Genomics Institute-Shenzhen, Shenzhen, China; and [14]Department of Medical-Surgical Physiopathology and Transplantation, University of Milan, Milan, Italy

Additional supporting information can be found in the online version of this article.

optic neuropathy, acting as recessive or phenotype-modifier variants. All the DOA-associated *AFG3L2* mutations were clustered in the ATPase domain, whereas SCA28-associated mutations mostly affect the proteolytic domain. The pathogenic role of DOA-associated *AFG3L2* mutations was confirmed in yeast, unraveling a mechanism distinct from that of SCA28-associated *AFG3L2* mutations. Patients' fibroblasts showed abnormal OPA1 processing, with accumulation of the fission-inducing short forms leading to mitochondrial network fragmentation, not observed in SCA28 patients' cells.

Interpretation: This study demonstrates that mutations in *AFG3L2* are a relevant cause of optic neuropathy, broadening the spectrum of clinical manifestations and genetic mechanisms associated with *AFG3L2* mutations, and underscores the pivotal role of OPA1 and its processing in the pathogenesis of DOA.

ANN NEUROL 2020;88:18–32

Introduction

Dominant optic atrophy (DOA) is a frequent optic neuropathy with infantile onset, affecting primarily the papillomacular bundle, leading to temporal pallor of the optic disc and loss of central vision with central scotoma, abnormal color vision, and relentless slow progression.[1,2]

In 2000, causative heterozygous variants in the *OPA1* gene (NM_130837.2) were reported,[3,4] and currently up to 70% of DOA patients worldwide are estimated to carry an *OPA1* mutation.[5] DOA prevalence may range from 1:12,000 to 1:25,000.[2,5,6] OPA1 is a multifunctional mitochondrial protein, expressed in 8 isoforms from alternative splicing of 3 exons (4, 4b, and 5b), further processed from long (L) to short (S) forms, due to 2 cleavage sites for the mitochondrial proteases YME1L (*i*-AAA) and OMA1.[7] The main function of OPA1 L and S forms is to drive and regulate fusion and fission of the inner mitochondrial membrane (IMM), respectively,[8] finely sensing the metabolic needs of the cells.[9] In regulating the dynamics of the IMM, OPA1 crucially shapes the structure of mitochondrial cristae and contributes the respiratory chain supercomplexes assembly.[10] Thus, *OPA1* mutations may result in defective oxidative phosphorylation in DOA patients.[11,12]

Most DOA-related *OPA1* mutations are predicted to lead to haploinsufficiency, whereas missense mutations are less frequent.[13] Some families are characterized by syndromic association of DOA with sensorineural deafness and chronic progressive external ophthalmoplegia, defined as DOA "plus."[14–16] Notably, compound heterozygous *OPA1* mutations have been described in a few cases manifesting complex neurological involvement in addition to optic atrophy.[13,17,18]

About 30% of DOA patients, however, do not carry *OPA1* mutations. Heterozygous mutations in a second gene, associated with DOA and cataracts and/or deafness, affect the *OPA3* gene,[19,20] known for the recessive Costeff syndrome (Online Mendelian Inheritance in Man database [OMIM] #258501). A third gene, carrying heterozygous mutations associated with DOA and deafness, is *WFS1,*[21] known for the recessive Wolfram syndrome (OMIM #222300), and a fourth gene associated with DOA is *DNM1L* (OPA5) encoding DRP1, a crucial protein involved in mitochondrial fission.[22]

More recently, heterozygous mutations in the *AFG3L2* gene were described in 3 unrelated patients with nonsyndromic[23,24] and syndromic[25] optic atrophy. *AFG3L2* encodes 1 of the 2 subunits—the other being SPG7/paraplegin—of the mitochondrial matrix AAA metalloprotease (*m*-AAA), an adenosine triphosphate (ATP)-dependent proteolytic complex located in the IMM, where it carries out protein quality control and participates in the processing and maturation of some mitochondrial proteins.[26–28] Heterozygous mutations in *AFG3L2* are known to cause autosomal dominant spinocerebellar ataxia 28 (SCA28),[29] whereas, rarely, homozygous *AFG3L2* mutations have been associated with a complex autosomal recessive spastic ataxia syndrome (SPAX5).[30]

Here, we report the identification of novel heterozygous mutations in *AFG3L2* in *OPA1*-negative DOA families or sporadic cases, presenting clinical features nearly indistinguishable from *OPA1*-related DOA. A few patients exhibited additional neurological symptoms, carrying compound heterozygous *AFG3L2* variants, suggestive of a recessive pattern of inheritance. To validate pathogenicity and elucidate the molecular basis of these mutations, we performed yeast and cellular studies, ultimately demonstrating altered OPA1 processing leading to excessive mitochondrial fragmentation as final pathogenic mechanism also in AFG3L2-associated optic atrophy.

Subjects and Methods

Genetic Screening

A cohort of subjects with isolated or syndromic optic neuropathy, negative for *OPA1* mutations, were investigated by different genetic screenings at 3 referral centers (Bologna, Milan, and Tübingen). All the procedures involving human subjects were approved by the institutional review boards. Each individual providing a biological sample signed informed consent. Genomic DNA was extracted from peripheral-blood lymphocytes using standard procedures.

Patients were screened by different next generation sequencing (NGS) approaches. Eighty-one index cases were

investigated by a panel including 35 genes (list available upon request) associated with genetic forms of optic atrophy. The amplicon-based NGS library (TruSeq Custom Amplicon; Illumina, San Diego, CA) was sequenced on Illumina MiSeq. Independently, 5 subjects (2 index cases and 3 additional subjects) from 2 families (Families 5 and 6) were analyzed by whole exome sequencing (WES; Agilent SureSelect Human All Exon 50 M; Agilent Technologies, Santa Clara, CA) on Illumina HiSeq. An additional 203 index cases were screened using a panel of genes associated with mitochondrial disorders, including optic atrophy (list available upon request). The capture-based NGS library (Nextera Rapid Capture Custom Kit, Illumina) was sequenced on Illumina MiSeq.

For bioinformatic analysis, reads were aligned to the human genome (hg19) and the identified variants were annotated (ANNOVAR) and filtered, focusing on rare variants (≤0.5% in public databases) causing potentially damaging changes (Combined Annotation Dependent Depletion, PolyPhen-2, DANN). Variant confirmation and segregation analysis were performed by Sanger sequencing.

Case Reports

Pedigrees are shown in Figure 1, and clinical features are summarized in the Table and Supplementary Table S1.

Family 1. The proband (I-1) is a 74-year-old male presenting slowly progressive visual loss manifesting with bilateral temporal pallor of the optic discs in his 50s. Lactic acid, electromyography, and brain magnetic resonance imaging (MRI) were normal, except for mineral deposits at basal ganglia. Audiometry revealed bilateral sensorineural deafness. Visual evoked potentials documented bilateral delayed latencies and reduced amplitude of cortical responses. Three other relatives were similarly affected.

Family 2. This is a large family, with several affected members. The proband (IV-1), a 60-year-old male, was diagnosed at 36 years with optic atrophy and glaucoma. His visual function progressively worsened. Two of the 3 proband's offspring (V-2, V-3) were mildly affected, whereas 1 (V-1) was clinically unaffected but with a mild temporal thinning of the retinal nerve fiber layer (RNFL).

Family 3. This sporadic case is a 15-year-old child who had been complaining of visual disturbances since childhood (6 years). Brain MRI showed atrophy of the optic nerves, chiasm, and optic tracts. He had intellectual disability, with more profound nonverbal (intelligence quotient [IQ] = 36) than verbal (IQ = 62) performance defect.

Family 4. The proband (III-1) is a 24-year-old male presenting visual disturbances since childhood (3 years). Lactic acid was normal. His father (II-1) presented both optic atrophy and bilateral sensorineural deafness.

Family 5. The proband (II-5) is a 74-year-old male. Since childhood, he had poor vision. At 60 years, he manifested slowly progressive ataxic–spastic gait and a mild hearing defect. Brain MRI displayed cerebellar atrophy, mild cerebral atrophy, and severe optic atrophy. Electromyography showed axonal neuropathy. At last examination, he showed blindness, with severe ophthalmoparesis and nystagmus, moderate hearing loss, mild speech impairment, generalized hypotonia without weakness, ataxic–spastic gait, and global hyperreflexia. Muscle respiratory chain activities were normal. The proband's father (I-1) and brother (II-1) were referred to have optic atrophy and hearing loss. The 47-year-old proband's son (III-5) had nystagmus and optic atrophy since early childhood (3 years). At last examination, hearing was normal and there were no signs of neurological involvement. He had severe visual loss with complete color blindness, very poor visual acuity (0.1), and pale optic discs. Optical coherence tomography (OCT) examination showed bilateral severely reduced RNFL thickness.

Family 6. Three individuals were affected with optic atrophy. The mother (I-2) first noticed visual reduction at 8 years of age, which remained mild until the current age of 65 years. At 55 years old, she first noticed a nonprogressive cervical dystonia, still responsive to botulinum toxin treatment 10 years later. Currently, she remains negative for signs of cerebellar ataxia, spasticity, myoclonus, or chorea. Her son (II-2) noticed reduced visual acuity since 4 years of age, which has been mildly progressive, with difficulties to read small letters at the current age of 40 years. Currently, he has no signs of cerebellar ataxia, spasticity, or other movement disorder. The daughter (II-1) showed optic atrophy since 2 years of age, which progressed after age 15 years, leading to bilateral blindness. She also had childhood myoclonus of the extremities since 8 years of age, and a progressive spastic–ataxic gait disorder since 15 years of age. At 35 years old, she showed blindness, a mild-to-moderate cerebellar ataxia (Scale for the Assessment and Rating of Ataxia [SARA] score = 7 points), paraspasticity, myoclonus of the extremities, and chorea of the hands. Ataxia progressed, and SARA score was 13.5 points at 43 years. The father (I-1) was subjectively asymptomatic. However, at 64 years old, he showed signs of ataxia, with a borderline SARA score of 4 points (cutoff > 3 points). No other neurological abnormalities were observed, and ophthalmological examination and brain MRI were negative.

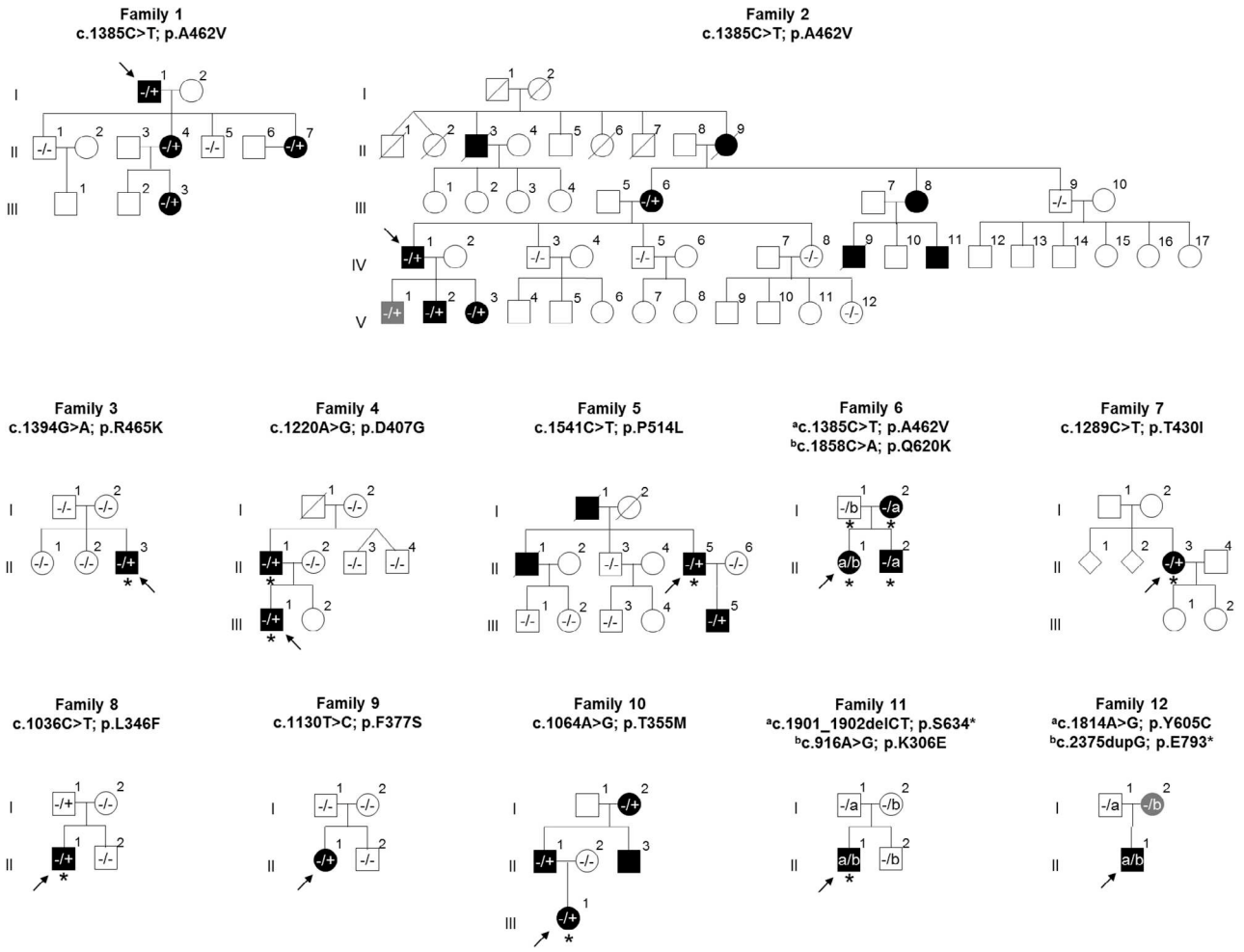

FIGURE 1: Pedigree of the 12 optic atrophy families with segregation of the identified *AFG3L2* variants. Black symbols indicate patients with optic neuropathy; gray symbols indicate subjects with subclinical phenotype. Arrows indicate family index cases. Asterisks indicate individuals manifesting optic atrophy along with adjunctive neurological findings (see details in the Table).

Family 7. A sporadic patient, a 39-year-old woman, presented visual loss starting 2 years previously. Optic nerves were reported normal on brain MRI. The neurological examination was normal except for a mild reduction of deep tendon reflexes.

Family 8. A sporadic patient, a 19-year-old male, presented visual loss since infancy. Brain MRI showed optic nerve hypotrophy. He showed diffuse optic disc pallor and size reduction of retinal arterial vessels. He had presented congenital nystagmus, spontaneously resolved at 10 years. His brother had normal vision. The father had no visual or neurological disturbances, but he did not undergo ophthalmological examination.

Family 9. A sporadic 11-year-old girl who had showed optic atrophy at age 9 years. Neurological examination was normal as well as brain computed tomography scan. OCT was normal in her parents and brother.

Family 10. The proband (III-1) is a 19-year-old girl. Family history was positive for early onset optic atrophy (II-1, II-3, and I-2). She had presented psychomotor delay. Optic atrophy was detected at 2 years. During childhood, she showed neurological signs of motor disturbance. At 15 years, brain MRI showed diffuse mild cerebral atrophy. At 18 years, neurological evaluation showed tetraparesis, bradykinesia, dystonia, and cognitive involvement.

Family 11. A sporadic patient, an 18-year-old male, presented at 4 years with walking difficulties and gait ataxia. He then developed involuntary hyperkinetic movements of the upper limbs and a dystonic posture. Visual deficit became evident at 9 years of age, and optic atrophy was detected. He now presents ataxia, dysmetria, dysarthria, and dystonia. At 6 years, MRI disclosed T2-hyperintensity of the putamen, pallidus, and substantia nigra; MRI follow-up showed caudate nuclei (11 years) and subthalamus (14 years) involvement. Ophthalmological evaluation was normal in the father (I-1), and the

TABLE. Genetic and Neuro-Ophthalmological Findings

Family	Identifier	Age, yr	*AFG3L2* Mutation		VA Reduction	Abnormal Color Vision	FO Pallor	OCT (decreased RNFL thickness)	Neurological Findings
F1	I-1	74	c.1385C > T	p.A462V	+	+	+	+	—
	II-4	49			−	+	+	+	—
	II-7	45			+	+	+	+	—
	III-3	29			+	+	+	+	—
F2	IV-1	60	c.1385C > T	p.A462V	+	+	+	+	—
	V-1	33			−	−	−	+	—
	V-2	32			+	+	+	+	—
	V-3	25			+	+	+	+	—
F3	II-3	15	c.1394G > A	p.R465K	+	+	+	+	Mild intellectual disability
F4	II-1	63	c.1220A > G	p.D407G	+	+	+	+	Sensorineural deafness
	III-1	24			+	+	+	+	Heterotopic cortical nodule adjacent to lateral left ventricle
F5	II-5	74	c.1541C > T	p.P514L	+	+	+	+	Spastic paraparesis
	III-5	47			+	+	+	+	—
F6	I-1	64	c.1858C > A	p.Q620K	−	−	−	−	Very mild ataxia, subjectively unnoticed
	I-2	65	c.1385C > T	p.A462V	−	+	+	+	Cervical dystonia
	II-1	36	c.1385C > T c.1858C > A	p.A462V p.Q620K	+	+	+	+	Ataxia, spasticity, myoclonus Distal chorea,
	II-2	40	c.1385C > T	p.A462V	+	+	+	+	depression
F7	II-3	39	c.1289C > T	p.T430I	−	−	+	+	Mild reduction of deep tendon reflexes
F8	II-1	19	c.1036C > T	p.L346F	+	+	+	+	Congenital nystagmus (spontaneously resolved)
F9	II-1	11	c.1130 T > C	p.F377S	+	+	+	+	—
F10	II-1	53	c.1064C > T	p.T355M	+	+	+	+	—
	III-1	19			ne	ne	+	ne	Hyperkinetic movements, cerebellar signs, dystonia
F11	I-1	57	c.1901_1902delCT	p.S634*	−	−	−	−	—
	I-2	58	c.916A > G	p.K306E	−	−	−	−	—
	II-1	18	c.1901_1902delCT c.916A > G	p.S634* p.K306E	+	+	+	+	Cerebellar signs and dystonia
F12	I-1	72	c.1814A > G	p.Y605C	−	−	−	−	—
	I-2	71	c.2375dupG	p.E793*	−	−	+	+	—
	II-1	42	c.1814A > G c.2375dupG	p.Y605C p.E793*	+	+	+	+	—

Variants refer to SeqRef NM_006796.3.
FO = fundus oculi; ne = not evaluable; OCT = optical coherence tomography; RNFL = retinal nerve fiber layer; VA = visual acuity.

mother (I-2) showed only a slight maculopathy unrelated to the son's pathology. Both parents were neurologically normal.

Family 12. This 42-year-old male was diagnosed with optic atrophy when he was 4 years old. Visual function remained stable. At 17 years, brain MRI and neurological examination were normal. The mother (I-2) was clinically normal, but OCT demonstrated a reduction of RNFL in the temporal quadrants. Except for amblyopia in the left eye, the father (I-1) was clinically asymptomatic, and the ophthalmologic examination confirmed a normal RNFL.

Yeast Studies

Five AFG3L2 variants (NM_006796.3) identified in patients (p.D407G, p.A462V, p.R465K, p.P514L, p.Q620K) were functionally studied in a yeast model, as previously described.[25,29] Fragments spanning the selected variants were generated by Invitrogen

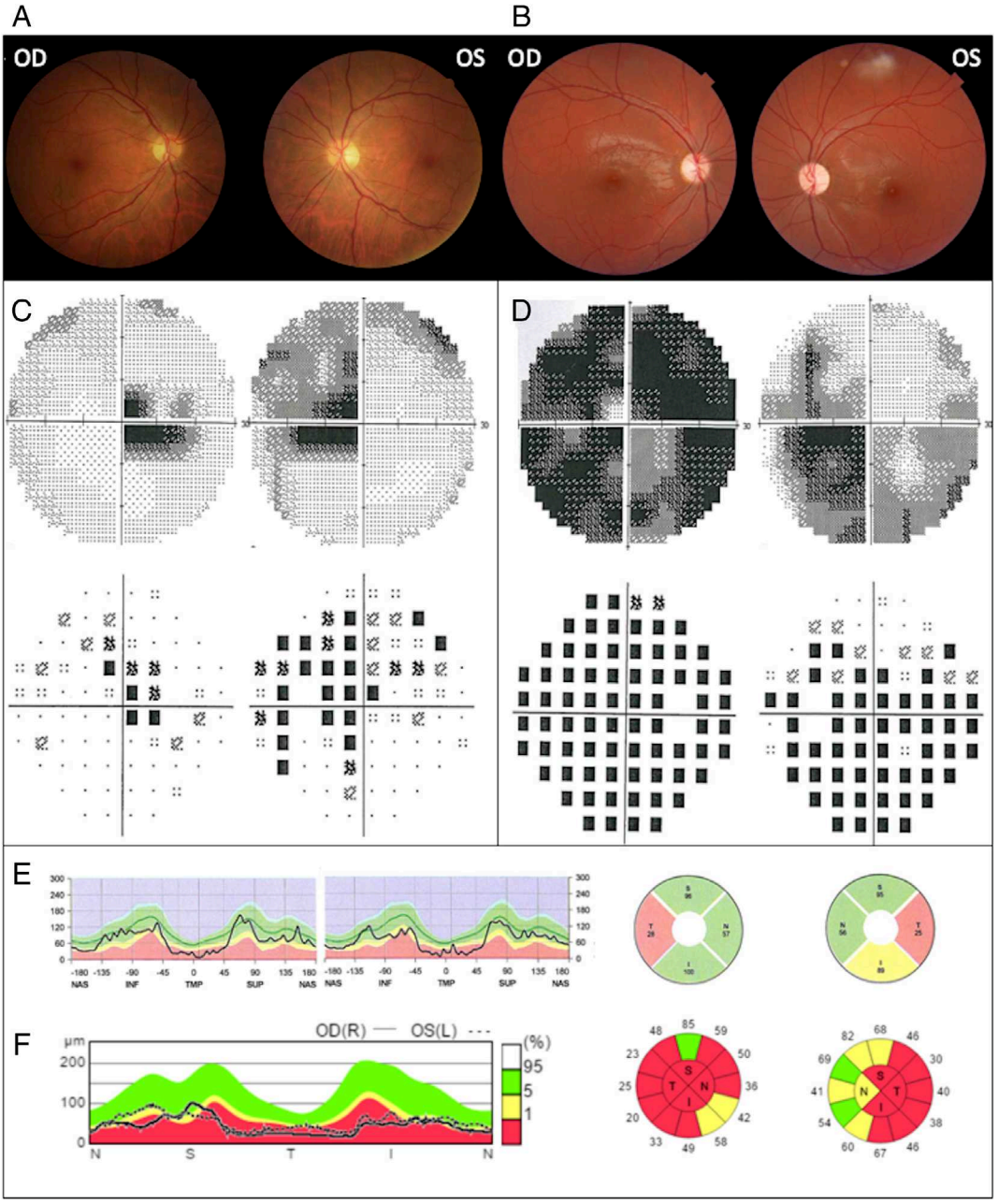

FIGURE 2: Ophthalmologic findings. Ophthalmologic features in 2 patients: a mild case (F2 IV-1; A, C, and E) and a severe case (F3 II-3; B, D, and F). For each case, fundus oculi (A, B), Humphrey visual fields 30–2 (C, D), and retinal nerve fiber layer (RNFL) thickness measurements on optical coherence tomography (E, F) are reported. The mild case displays only a temporal pallor at fundus oculi, which congruently corresponds to central scotoma, and a selective temporal loss of RNFL thickness. The severe case presents with generalized pallor of the optic disk, widespread loss of sensitivity at visual field, and global loss of RNFL thickness. I,INF = inferior; L = left; N,NAS = nasal; OD = "Oculus Dexter" or right eye; OS = "Oculus Sinister" or left eye; R = right; S,SUP = superior; T,TMP = temporal.

(Carlsbad, CA) GeneArt Gene Synthesis and cloned into the yeast construct pYC6/CT-ADH1-AFG3L2-V5.[29] All strains used in this study were obtained transforming the double-knockout yeast strain (*yta10Δyta12Δ*) derived from strain W303 with AFG3L2 (NM_006796.3) and paraplegin (SPG7, NM_003119.3) expression plasmids.[25,29]

Fibroblast Cell Culture

Skin fibroblasts were derived from 2 unrelated healthy donors and 6 optic atrophy patients from 3 families. Fibroblasts were grown in Dulbecco modified Eagle medium (DMEM) medium supplemented with 10% fetal bovine serum, 2mM L-glutamine, and antibiotics. For the experiments, we used DMEM glucose medium or DMEM glucose-free medium containing 5mM galactose and 5mM pyruvate.[31]

Immunoblot Analysis

Immunoblot analysis of AFG3L2, Ccp1, MrpL32, paraplegin, and OPA1, using actin, HSP60, or MTPα as loading controls, was performed on yeast cells or patient-derived fibroblasts as previously described.[29]

Mitochondrial Network Morphology

The mitochondrial fluorescent dye MitoTracker Red-CMXRos (Invitrogen) was used to visualize the mitochondrial network in live cells, and circularity of mitochondria was calculated using the image processing package ImageJ (Fiji).[32]

Alternatively, mitochondrial network was labeled with the anti-TOM20 antibody and cells were classified by blind test into 3 categories as follows: filamentous, intermediate, and fragmented mitochondria.[31]

Oxygen Consumption Studies

The oxygen consumption rate (OCR) was measured using XF 24-well or XF 96-well cell culture microplates (Seahorse Bioscience, Billerica, MA) as previously described.[31,33]

Statistical Analyses

The data were analyzed by 1-way analysis of variance with Dunnett multiple comparisons test and unpaired 2-tailed *t* test, using Prism version 6.07 (GraphPad Software, San Diego, CA). Differences between groups were considered to be significant at $p < 0.05$.

Data Availability

Supporting data for this study are available from the corresponding authors upon request.

Results

Genetic Analysis Reveals Mutations in AFG3L2

We screened a total of 286 index cases presenting optic atrophy and negative for *OPA1* mutations. We identified 12 probands harboring *AFG3L2* variants: 10 of 284 by disease-related (optic atrophy and mitochondrial disorders) multigene panels and 2 by WES. Overall, these results indicate a frequency of ~4% in our *OPA1*-negative optic atrophy cohort. Six of 12 index cases are familial cases with an autosomal dominant pattern of inheritance (F1, F2, F4, F5, F6, and F10), whereas six (F3, F7, F8, F9, F11, and F12) are sporadic. From the 12 families, a total of 24 affected subjects with *AFG3L2* variants were identified (see Fig 1). A

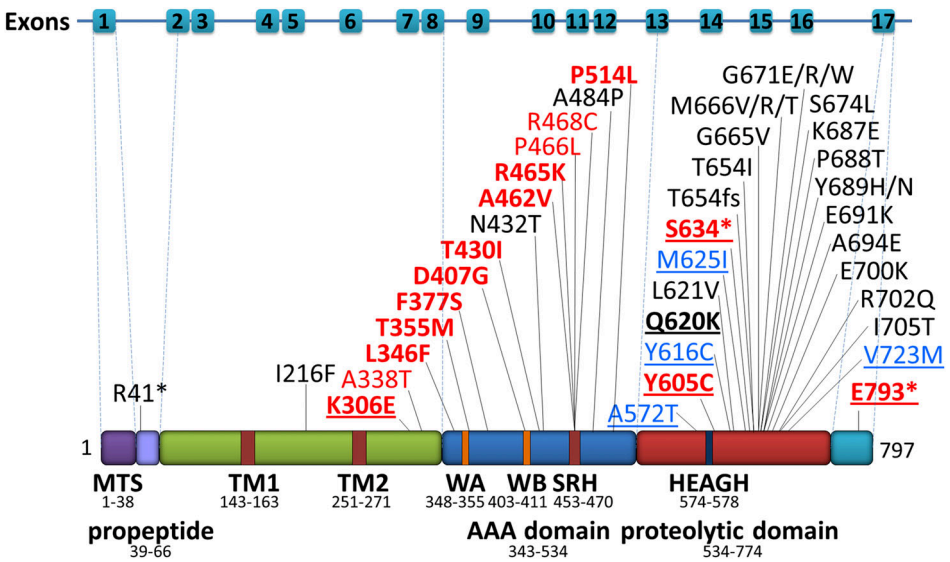

FIGURE 3: Mutation distribution on AFG3L2 protein. *AFG3L2* (NM_006796.3) pathogenic variants associated with optic atrophy (red), spinocerebellar ataxia 28 (SCA28; black), and spastic ataxia syndrome 5 (SPAX5; blue) phenotypes. Details and references are reported in Supplementary Table 2. Variants reported in this study are in bold. Biallelic variants are underlined. The distribution of pathogenic variants associated with isolated optic atrophy, which are predominantly located in the ATPase domain, is distinct from those associated with SCA28 and SPAX5, which are mainly located in the proteolytic domain.

summary of neuro-ophthalmological and neurological phenotype is reported in the Table and Supplementary Table S1, and the neuro-ophthalmological features in 2 patients from 2 families (F2 IV-1 and F3 II-3) are depicted as an example in Figure 2.

Nine families (F1–F5 and F7–F10) harbored a single heterozygous missense variant, with an autosomal dominant pattern of inheritance in 5 cases (p.A462V, F1 and F2; p.D407G, F4; p.P514L, F5; p.T355M, F10) and a sporadic presentation in the remaining. Among these, 2 variants were de novo (p.R465K, F3 and p.F377S, F9), 1 was inherited from an asymptomatic father (p.L346F, F8), suggesting reduced penetrance or a subclinical phenotype, and 1 (p.T430I, F7) was detected in the only affected member of the family, with no genetic data available from the relatives.

In 2 families, the index case carried biallelic variants, with a missense change in compound heterozygosity with a frameshift mutation (p.K306E + p.S634* in F11 and p.Y605C + p.E793* in F12). In both cases, the disease clinically manifested in the compound heterozygotes only, which would suggest a recessive inheritance pattern.

Finally, Family 6 exhibited a more complex genotype, with 2 heterozygous *AFG3L2* missense variants, p.A462V and p.Q620K. Interestingly, individuals harboring p.A462V only (F6 I-2 and II-2) exhibited a pure optic atrophy phenotype (with only mild late onset cervical dystonia in F6 I-2), whereas patient F6 II-1, carrying both p.A462V and p.Q620K, had a more complex phenotype characterized by optic atrophy, severe childhood onset ataxia, spasticity, and generalized dystonia. The father

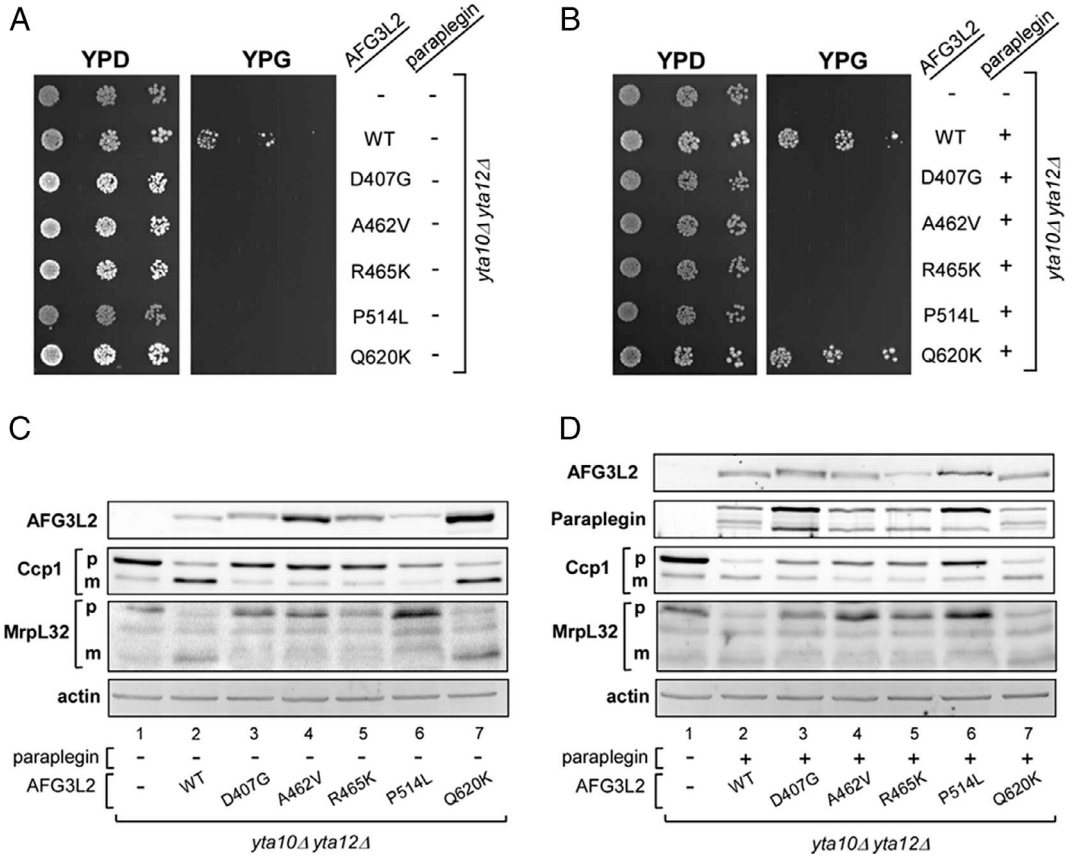

FIGURE 4: Studies in yeast cells expressing mutant human AFG3L2. Respiratory phenotype of *yta10Δyta12Δ* yeast cells expressing normal and mutant human AFG3L2 is shown. Serial dilutions of normalized yeast cultures were spotted on YEP plates containing 2% glucose (YPD) or 2% glycerol (YPG) and incubated at 28°C for 3 days. Respiratory competence was deduced by the ability to grow on 2% glycerol (YPG). (A) Respiratory phenotype of K699 (wild-type [WT] yeast strain) and *yta10Δyta12Δ* cells expressing either normal (WT) AFG3L2 or AFG3L2 carrying the mutations indicated. (B) Respiratory phenotype of K699 and *yta10Δyta12Δ* cells coexpressing either normal or mutant human AFG3L2 with human paraplegin. Dislocase (ATPase) and proteolytic activity of normal and mutant human AFG3L2 in yeast is shown. (C, D) Fluorescence immunoblot analysis of Ccp1 and MrpL32 precursor (p) and mature (m) forms in yeast cells expressing either normal (WT) or mutant human AFG3L2 alone (C) and coexpressed with paraplegin (D). Dislocase (ATPase) and proteolytic competence is assessed by precursor accumulation of Ccp1 and MrpL32, respectively. The slightly larger size of AFG3L2 observed in lanes 3–6 of C and D indicates defective autocatalytic processing[25,48] due to the proteolytic defect of mutants p.D407G, p.A462V, p.R465K, and p.P514L. β-Actin was used as loading control in C and D. YEP plates = yeast growth medium composed of Yeast Extract and bacto-Peptone.

(F6 I-1), carrying p.Q620K, was subjectively asymptomatic, showing only borderline signs of mild ataxia at neurological examination and no clinical signs of optic atrophy at the age of 64 years.

All the identified variants are not reported in the gnomAD database (https://gnomad.broadinstitute.org). All dominant variants associated with pure optic atrophy (8/11) affect amino acid residues, evolutionarily conserved from bacteria to humans (not shown), in the AAA domain (ATPase domain; Fig 3).

Yeast Model Confirms the Pathogenicity of the Identified AFG3L2 *Variants*

The functional effect of 5 representative missense substitutions identified in our cohort of patients was assessed using the yeast model previously described.[29] In particular, we functionally tested 4 variants affecting the ATPase domain and associated with optic atrophy phenotype (p.D407G, p.A462V, p.R465K, p.P514L) and the variant p.Q620K that affects the proteolytic domain and is associated with a complex phenotype when in compound heterozygosity with p.A462V (F6 II-1).

Human AFG3L2 protein carrying these variants was expressed in a yeast strain defective for *YTA10* and *YTA12,* the yeast orthologs of human AFG3L2 and paraplegin, respectively (*yta10Δyta12Δ*). Complementation studies with wild-type AFG3L2 and the 5 variants showed that the respiratory defect (oxidative phosphorylation [OXPHOS] phenotype) of *yta10Δyta12Δ* was rescued by wild-type AFG3L2, but not by mutant AFG3L2, demonstrating a deleterious effect of all these variants on the function of AFG3L2 homocomplex (Fig 4A). Moreover, to evaluate the variant effect on the AFG3L2/paraplegin heterocomplex, wild-type and mutant AFG3L2 were coexpressed along with paraplegin (see Fig 4B). Strains carrying p.D407G, p.A462V, p.R465K, and p.P514L AFG3L2 variants along with paraplegin exhibited an OXPHOS phenotype. Interestingly, paraplegin coexpression in the strain carrying the p.Q620K variant completely rescued the respiratory defect.

Furthermore, to evaluate the variant effect on the proteolytic and dislocase activity of the *m*-AAA complexes, we tested the processing of 2 known substrates of yeast *m*-AAA, the ribosomal subunit MrpL32[27] and the reactive oxygen species (ROS) scavenger protein Ccp1.[26] In

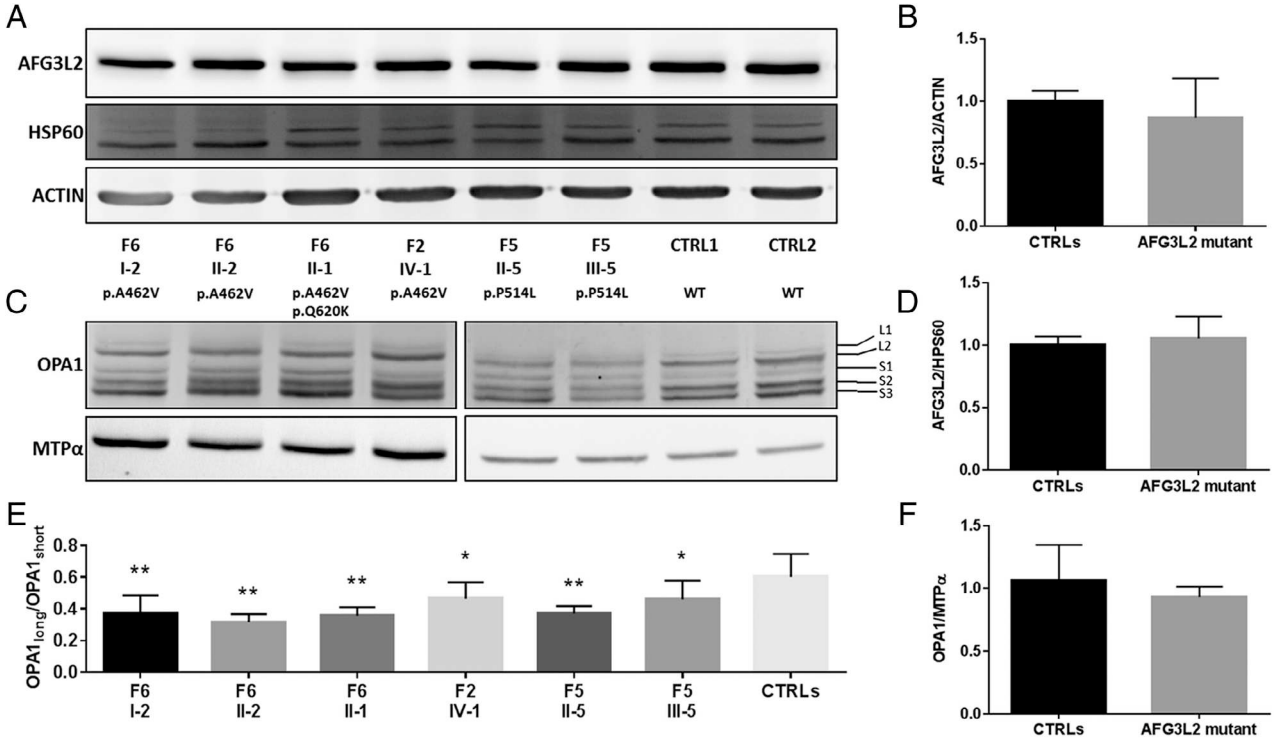

FIGURE 5: AFG3L2 and OPA1 analysis in patients' fibroblasts. Protein expression in fibroblasts derived from 6 probands from 3 families (F2 IV-1; F5 II-5, III-5; F6 I-2, II-1, II-2) and controls are displayed; for each sample, family and subject identifier as well as the AFG3L2 mutation are indicated. (A) Western blot of AFG3L2 expression levels. (B) Actin was used as a loading control. (C) Western blot of OPA1 expression levels, with indication of long (L1, L2) and short (S1, S2, S3) bands; MTPα was used as a loading control. (D) HPS60 was used as mitochondrial mass indicator. (E-F) Densitometric analysis of C shows a reduction of $OPA1_{long}/OPA1_{short}$ ratio in all fibroblasts carrying *AFG3L2* mutations (E) with no change in the total amount of OPA1 (F). Data, normalized to the control cells, are mean ± standard deviation of 3 independent experiments. Statistical analysis was performed by 1-way analysis of variance with Dunnett multiple comparisons test. Asterisks indicate statistical significance (*adjusted $p < 0.05$, **adjusted $p < 0.001$).

particular, the conversion of MrpL32 from precursor to mature form is an indicator of the overall proteolytic competence, whereas the maturation of Ccp1 indicates the ATP-dependent capacity of *m*-AAA complex to dislocate proteins from the inner mitochondrial membrane (dislocase activity).[34,35] In strains carrying the p.D407G, p.A462V, p. R465K, and p.P514L AFG3L2 variants, both Ccp1 and MrpL32 accumulate as precursor, suggesting that these variants abolished both the ATPase-dependent dislocase activity and the proteolytic competence (see Fig 4C, lanes 3–6). By contrast, p.Q620K AFG3L2 is able to normally process both Ccp1 and MrpL32 (compare lanes 7 and 2 in Fig 4C),

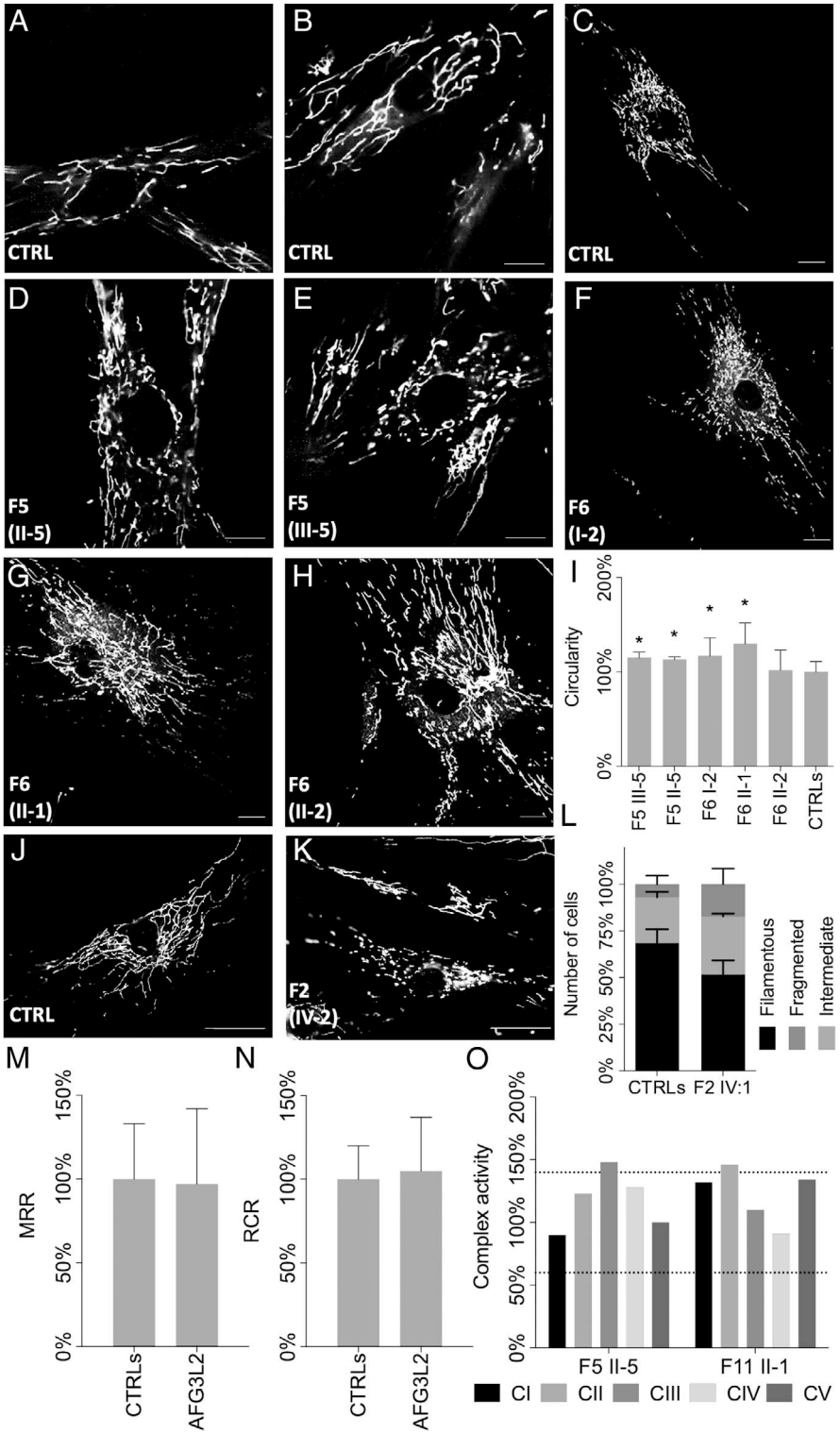

(Figure legend continues on next page.)

indicating that this AFG3L2 mutant substantially maintains both proteolytic and ATPase (dislocase) activity.

In yeast cells expressing *m*-AAA heterocomplexes constituted by wild-type or mutant AFG3L2 and paraplegin (see Fig 4D), the processing pattern of Ccp1 and MrpL32 is the same as in the presence of the homocomplex (see Fig 4C).

Taken together, these results demonstrate that all the tested variants affect AFG3L2 function, confirming their pathogenic role. Notably, the variants located in the ATPase domain (p.D407G, p.A462V, p.R465K, and p.P514L) affect also the heterocomplex function and show a defect in both proteolytic and dislocase activity. By contrast, the p.Q620K variant causes a respiratory defect (see Fig 4A) but shows no alteration in processing these substrates and is rescued by paraplegin coexpression, thus representing a paraplegin-responsive mutation as the majority of *AFG3L2* mutations causing SCA28 previously tested.[29]

Cell Studies Demonstrate Alteration of OPA1 Processing

To evaluate the effect of the missense *AFG3L2* mutations in a human context, we analyzed skin fibroblasts from 6 patients from 3 families (F2 IV-1; F5 II-5, III-5; F6 I-2, II-1, II-2). Immunoblot analysis did not show any significant reduction in the expression level of AFG3L2 protein in mutant fibroblasts compared to controls (Fig 5A, B, D). We also assessed OPA1 expression; although the total amount of OPA1 protein was similar in patients and control cells (see Figure 5C-F), we observed a significant reduction of L form (L1 + L2) to S form (S1 + S2 + S3) ratio (see Fig 5C–E), suggesting an increased proteolytic cleavage of long forms of OPA1 and accumulation of short forms.

Altered Mitochondrial Network in Fibroblasts with AFG3L2 *Mutations*

Because balance of short and long OPA1 forms is required for mitochondrial fusion activity in mammals,[36] we investigated the fibroblast mitochondrial network by morphometric analyses in fibroblasts from 5 affected members from 2 families (F5 II-5, III-5; F6 I-2, II-1, II-2). Fibroblasts were grown in galactose medium for 48 hours, stained with fluorescent dye. Overall, we observed a significant fragmentation of mitochondrial network in patients' fibroblasts, as demonstrated by higher circularity values compared to controls, with the most altered network in the subject harboring biallelic *AFG3L2* mutations (F6 II-1; Fig 6A–I).

Mitochondrial fragmentation was also observed in fibroblasts from a Family 2 patient (IV-1; see Fig 6J–L). Fibroblasts were grown in DMEM glucose or galactose medium, stained with a mitochondrial marker (TOM20), fixed, and then scored into 3 categories (filamentous, intermediate, fragmented). In glucose medium, both control and patient's fibroblasts exhibited a similar percentage of cells with filamentous and intermediate mitochondria (data not shown). After 48-hour incubation in galactose medium, *AFG3L2* mutant fibroblasts significantly increased the percentage of intermediate and fragmented mitochondria (see Fig 6J–L), as observed in fibroblasts from patients with *OPA1* mutations.[11,31] By contrast, mitochondrial morphology in control fibroblasts was similar in both growth conditions.

Despite the alterations in mitochondrial network, measurement of OCR levels (F2 IV-1; F5 II-5, III-5; F6 I-2, II-1, II-2) did not reveal reduction of energetic competence of *AFG3L2* mutant fibroblasts compared to controls (see Fig 6M, N). Congruently, assessment of OXPHOS complex activity was within normal range in muscle biopsies available from 2 patients, F5 II-5 and F11 II-1 (see Fig 6O).

Discussion

This study demonstrates that heterozygous mutations in *AFG3L2* are a relevant cause of optic atrophy in *OPA1*-negative DOA, impacting about 4% in our cohort. Remarkably, the large majority of these mutations affected the AAA (ATPase) domain, in contrast to the *AFG3L2*

FIGURE 6: Morphology of mitochondrial network in patients' fibroblasts. (A–H, J, K) Analysis of mitochondrial morphology in live cells with the mitochondrial dye MitoTracker Red-CMXRos (A–H) and in fixed cells labeled with the anti-Tom-20 (J-K), by fluorescence microscopy in control (n = 4) and patient (n = 6) fibroblasts, incubated in Dulbecco modified Eagle medium–galactose for 48 hours. Representatives images are shown for each cell line: controls (A, B, C); Family 5 II-5 (D) and III-5 (E); Family 6 I-2 (F), II-1 (G), and II-2 (H); control (J); and Family 2 IV-1 (K). Scale bars = 25μm. Analysis of the mitochondrial shape factors (circularity) are reported in the graphs. (I) Data (mean ± standard deviation) are presented as percentage compared to controls. (L) Quantitative analysis of mitochondrial morphology classified as fragmented (dark gray), intermediate (light gray), and filamentous (black). Patients' fibroblasts display a fragmented mitochondrial network. (M, N) Mitochondrial bioenergetics analysis. Oxygen consumption rate was measured by Seahorse in basal condition and after injection of 1μM oligomycin, 1μM carbonyl cyanide-4-(trifluoromethoxy)phenylhydrazone, 1μM rotenone, and/or 1μM antimycin A. The oxygen consumption rate values (pmol·O_2^{-1}·min^{-1}) were normalized either for protein content, as determined by the sulforhodamine B assay,[31] or for cells number, as determined by CyQuant (Invitrogen). The analysis was carried out on fibroblasts from 2 controls and 6 patients (Family 2: IV-1; Family 5: II-5, F5 III-5; Family 6: I-2, II-1, II-2) expressed as maximum respiration rate (MRR; M) and respiratory control ratio (RCR; N). (O) Activities of mitochondrial respiratory chain complexes in muscle biopsies from Patients F5 II-5 and F11 II-1. Dashed lines indicate range of controls activity. Statistical analysis was performed by unpaired 2-tailed *t* test. Asterisks indicate statistical significance (*$p < 0.01$).

mutations associated with SCA28 and SPAX5 phenotypes, which are clustered in the proteolytic domain (see Fig 3). In some peculiar families, probands carried biallelic *AFG3L2* mutations inherited from heterozygous parents, leading to more complex phenotypes. In these cases, optic atrophy remains the major feature, but adjunctive central nervous system involvement of variable severity was observed, including the extreme case of a Leigh-like phenotype (F11 II-1). Modeling 5 *AFG3L2* mutations in yeast clearly defined their pathogenic potential. Moreover, investigation of patient-derived fibroblasts revealed an altered processing of long to short OPA1 isoforms, with a slight excess of short forms. This was consistently reflected in the hyperfragmented mitochondrial network, when cells were forced to use OXPHOS in galactose medium, a condition that limits the availability of ATP production by glycolysis. Ultimately, our findings suggest that the unbalanced processing of OPA1 consequent to AFG3L2 dysfunction possibly leads to the optic atrophy phenotype, thus providing the first insights into the mechanistic basis underlying this phenotypic cluster. The defective mitochondrial dynamics[3,4] fits well with the general paradigm of the pathogenic mechanism for mitochondrial optic neuropathies.

The current study expands on previous case reports on single patients with optic atrophy associated with mutations in the 2 components, AFG3L2 and SPG7/paraplegin, of *m*-AAA protease: 2 patients with a heterozygous *AFG3L2* mutation (p.R468C) in the ATPase domain associated with nonsyndromic optic atrophy[23,24]; 1 patient with early onset optic atrophy, spastic ataxia, and L-dopa–responsive parkinsonism, heterozygous for both the *AFG3L2* p.R468C mutation and an intragenic deletion in the *SPG7* gene[25]; and a single family with DOA associated with *SPG7* heterozygous mutation.[37] Furthermore, a homozygous mutation in the *YME1L1* gene, encoding 1 of the 2 proteases known to process OPA1, was found to cause infantile onset developmental delay, muscle weakness, ataxia, and optic atrophy.[38] Thus, the genetic landscape of optic atrophy, including syndromic ("plus") phenotypes, is expanded to include a new class, the AAA proteases involved in mitochondrial protein quality control. Notably, dominant, recessive, biallelic, or digenic inheritance patterns may occur.

SPG7 and *AFG3L2* encode the cognate subunits of the mitochondrial *m*-AAA protease complex, which carries out protein quality control by degrading nonassembled or damaged proteins of the IMM. It has been proposed that *m*-AAA loss may lead to overaccumulation of de novo synthesized proteins in the IMM, which in turn would cause mitochondrial membrane potential dissipation and stress-activation of the OMA1 metalloprotease that processes the long OPA1 isoforms to the shortest ones.[40] An abnormal processing pattern of OPA1 has been observed in cells from the patient with concurrent *AFG3L2* and *SPG7* mutations associated with early onset optic atrophy and a complex neurological phenotype.[25] Our current results in patient-derived fibroblasts carrying distinct *AFG3L2* mutations provide conclusive evidence that *m*-AAA protease activity impinges on OPA1 processing, which ultimately affects mitochondrial dynamics, thus presenting a common hub and key function for optic nerve maintenance.

Similarly, mice lacking *Afg3l2* exhibit fragmented mitochondrial network, leading to neurodegeneration.[41] This was proposed to be due to impaired metabolism of OPA1, which mediates mitochondrial fusion.[42] Evidence of a pathologic effect of mutant *SPG7* on optic nerve has been also provided in *Spg7*-deficient mice, documenting ultrastructural mitochondrial abnormalities and hyperfragmentation of the mitochondrial network,[43] features resembling those seen in postmortem tissues from patients with DOA or Leber hereditary optic neuropathy.[1] Interestingly, patients with biallelic *SPG7* mutations showed increased mitochondrial biogenesis with hyperfused mitochondria,[44] as did the recently described patients with *DNM1L* mutation.[22] This latter study demonstrates that optic neuropathy may result from impairment of either fusion or fission, both leading to opposite profound dysfunction of mitochondrial dynamics.[45] The impairment of the finely tuned mitodynamic processes affects mitochondrial morphology, bioenergetic efficiency, and ultimately mitochondrial biogenesis and maintenance.[46]

Remarkably, all the dominant *AFG3L2* mutations associated with optic atrophy affect the ATPase domain, in sharp contrast with those associated with SCA28 or SPAX5, which affect the proteolytic domain (see Fig 3, Supplementary Table 2).[47] Notably, the SPG7 mutation p.D411A reported to segregate with isolated DOA is also located in the AAA domain and is predicted to interfere with ATP binding/hydrolysis, ultimately impairing proteolytic activity.[37] Recently, using an atomic model of the human AFG3L2 homohexameric *m*-AAA protease trapped in the act of processing substrate, it has been demonstrated that clustering of AFG3L2 disease-associated mutations into distinct regions in the structure correlates with distinct effects on the mechanism of AFG3L2.[47] Consistent with this model, functional analysis in yeast (see Fig 4) demonstrated that DOA-associated *AFG3L2* mutations (p.D407G, p.A462V, p.R465K, and p.P514L) drastically impair both the ATPase-dependent dislocase activity, essential for the processing of membrane proteins, and the proteolytic competence of AFG3L2, including its autocatalytic processing.[48] By contrast, the SCA28 mutations, which affect the proteolytic domain, do not significantly alter the dislocase activity.[25,29] From this standpoint, the second *AFG3L2* mutation identified in Family 6 (p.Q620K, located in the proteolytic domain) resembles a mild SCA28 mutation, which corresponds

perfectly to the mild late onset ataxia phenotype observed in the heterozygous p.Q620K subject from this study (F6 I-1). However, although the p.Q620K clearly impairs yeast respiration, it does not significantly affect substrate processing. Furthermore, it is rescued by paraplegin coexpression, as observed in most SCA28 mutations[25,29] (S. Magri and F. Taroni, unpublished observation) but not in DOA mutations.[25] Consistently, the Family 6 member carrying this variant alone (F6 I-1) did not exhibit any ophthalmological symptoms, but only a very mild late onset ataxia that he was not even subjectively aware of at age 64 years. According to the structural model,[47] all the DOA mutations identified in our patients' cohort cluster in regions of the ATPase domain linked to 3 distinct functions: (1) ATP binding (Walker A and arginine finger: p.L346F, p.T355M, p.A462V, and p.R465K), (2) ATP hydrolysis (Walker B and α5: p.D407G and p.T430I), and (3) substrate interaction (p.F377S). Overall, our results conclusively demonstrate that *AFG3L2* mutations with clearly distinct biochemical impact account for the different patient phenotypes (ie, SCA28 vs DOA). Further evidence indicating that variants associated with SCA28 behave differently from those reported in the present article comes from a recently described knock-in SCA28 mouse model carrying a patient-derived missense mutation (p.M665R) in the AFG3L2 proteolytic domain, which shows mitochondrial fragmentation and increased OPA1 processing from long to short isoforms in cerebellum and brain, but not in optic nerves.[49]

Interestingly, 3 families (F6, F11, and F12) harbored *AFG3L2* biallelic mutations. In Families 11 and 12, the 2 sporadic patients were compound heterozygous for a missense change located outside the ATPase domain (p.K306E or p.Y605C) and a frameshift mutation (p.S634* or p.E793*). Because the heterozygous parents were clinically unaffected, these 4 variants likely represent hypomorphic/recessive mutations. By contrast, in dominant Family 6, the 2 subjects (I-2 and II-2) harboring the recurrent p.A462V variant alone present with optic atrophy, whereas the patient (II-1) compound heterozygous for pA462V and p.Q620K exhibits a severe childhood onset optic atrophy "plus" phenotype. The only very mild late onset clinical symptoms in the subject carrying p.Q620K alone (F6 I-1) indicates that this variant may act as a hypomorphic variant, with a strong effect as a phenotypic modifier, a notion that resembles findings from OPA1, where also hypomorphic variants act as intralocus phenotypic modifiers causing severe childhood onset multisystemic optic atrophy phenotypes.[17,50]

In conclusion, our study expands the landscape of genetic causes leading to optic atrophy, elucidates the underlying molecular mechanisms, and describes the general paradigm of specific vulnerability of retinal ganglion cells to mitochondrial dysfunction, with common clinical features undistinguishable from those known for the most common DOA caused by *OPA1* mutations. Furthermore, our results provide conclusive evidence that OPA1 is the key player in the pathogenesis of optic nerve degeneration, and its processing is a crucial step that involves the entire set of mitochondrial AAA proteases, either directly (*i*-AAA: YME1L) or indirectly (*m*-AAA: AFG3L2 and SPG7). Finally, this study illustrates the broad spectrum of clinical manifestations and genetic mechanisms (dominant, dominant de novo, recessive) associated with *AFG3L2* mutations and indicates that this gene shall be included in the diagnostic algorithm for both pure and syndromic optic neuropathies.

Acknowledgment

The "Cell Line and DNA Bank of Genetic Movement Disorders and Mitochondrial Diseases" of the Telethon Network of Genetic Biobanks (grant GTB12001J) and the EurobiobanK Network supplied biological specimens. This work was supported by the Telethon Foundation (grant GGP15041 to D.G.), the E-Rare project GENOMIT (to C.L.), the Pierfranco and Luisa Mariani Foundation, the Italian Ministry of Health (grants GR-2016-02361449 to L.C., RF-2011-02351165 and RF-2018-12367768 to F.Tar., and GR-2016-02363337 to S.M., and "Ricerca Corrente" funding to V.C.), the Horizon 2020 research and innovation program (grant 779257 "Solve-RD" to R.S. and M.S.), and the NIH (grant 5R01NS072248 to R.S.).

Author Contributions

L.C., S.M., D.G., V.C., and F.Tar. conceived and designed the study; L.C., S.M., A.L., V.D.D., F.Tag., F.B., A.N., C.L.M., M.Car., M.L.V., E.L., S.B., L.S., R.S., P.B., M.L.C., A.M., M.Cap., A.A., D.P., G.C., L.M., M.Z., L.P., C.L., S.B.M., M.F., M.S., and D.G., contributed to the acquisition and analysis of data; L.C., S.M., D.G., V.C., and F.Tar. drafted the text and prepared the figures.

Potential Conflicts of Interest

Nothing to report.

References

1. Carelli V, Ross-Cisneros FN, Sadun AA. Mitochondrial dysfunction as a cause of optic neuropathies. Prog Retin Eye Res 2004;23:53–89.

2. Yu-Wai-Man P, Griffiths PG, Chinnery PF. Mitochondrial optic neuropathies—disease mechanisms and therapeutic strategies. Prog Retin Eye Res 2011;30:81–114.

3. Alexander C, Votruba M, Pesch UE, et al. OPA1, encoding a dynamin-related GTPase, is mutated in autosomal dominant optic atrophy linked to chromosome 3q28. Nat Genet 2000;26:211–215.

4. Delettre C, Lenaers G, Griffoin JM, et al. Nuclear gene OPA1, encoding a mitochondrial dynamin-related protein, is mutated in dominant optic atrophy. Nat Genet 2000;26:207–210.
5. Lenaers G, Hamel C, Delettre C, et al. Dominant optic atrophy. Orphanet J Rare Dis 2012;7:46.
6. Yu-Wai-Man P, Chinnery PF. Dominant optic atrophy: novel OPA1 mutations and revised prevalence estimates. Ophthalmology 2013; 120:1712–1712.e1.
7. Anand R, Wai T, Baker MJ, et al. The i-AAA protease YME1L and OMA1 cleave OPA1 to balance mitochondrial fusion and fission. J Cell Biol 2014;204:919–929.
8. MacVicar T, Langer T. OPA1 processing in cell death and disease—the long and short of it. J Cell Sci 2016;129:2297–2306.
9. Mishra P, Carelli V, Manfredi G, Chan DC. Proteolytic cleavage of Opa1 stimulates mitochondrial inner membrane fusion and couples fusion to oxidative phosphorylation. Cell Metab 2014;19:630–641.
10. Cogliati S, Frezza C, Soriano ME, et al. Mitochondrial cristae shape determines respiratory chain supercomplexes assembly and respiratory efficiency. Cell 2013;155:160–171.
11. Zanna C, Ghelli A, Porcelli AM, et al. OPA1 mutations associated with dominant optic atrophy impair oxidative phosphorylation and mitochondrial fusion. Brain 2008;131:352–367.
12. Lodi R, Tonon C, Valentino ML, et al. Defective mitochondrial adenosine triphosphate production in skeletal muscle from patients with dominant optic atrophy due to OPA1 mutations. Arch Neurol 2011; 68:67–73.
13. Ferré M, Caignard A, Milea D, et al. Improved locus-specific database for OPA1 mutations allows inclusion of advanced clinical data. Hum Mutat 2015;36:20–25.
14. Amati-Bonneau P, Valentino ML, Reynier P, et al. OPA1 mutations induce mitochondrial DNA instability and optic atrophy "plus" phenotypes. Brain 2008;131:338–351.
15. Yu-Wai-Man P, Griffiths PG, Gorman GS, et al. Multi-system neurological disease is common in patients with OPA1 mutations. Brain 2010;133:771–786.
16. Carelli V, Musumeci O, Caporali L, et al. Syndromic parkinsonism and dementia associated with OPA1 missense mutations. Ann Neurol 2015;78:21–38.
17. Bonifert T, Karle KN, Tonagel F, et al. Pure and syndromic optic atrophy explained by deep intronic OPA1 mutations and an intralocus modifier. Brain 2014;137:2164–2177.
18. Nasca A, Rizza T, Doimo M, et al. Not only dominant, not only optic atrophy: expanding the clinical spectrum associated with OPA1 mutations. Orphanet J Rare Dis 2017;12:89.
19. Reynier P, Amati-Bonneau P, Verny C, et al. OPA3 gene mutations responsible for autosomal dominant optic atrophy and cataract. J Med Genet 2004;41:e110.
20. Grau T, Burbulla LF, Engl G, et al. A novel heterozygous OPA3 mutation located in the mitochondrial target sequence results in altered steady-state levels and fragmented mitochondrial network. J Med Genet 2013;50:848–858.
21. Rendtorff ND, Lodahl M, Boulahbel H, et al. Identification of p. A684V missense mutation in the WFS1 gene as a frequent cause of autosomal dominant optic atrophy and hearing impairment. Am J Med Genet A 2011;155A:1298–1313.
22. Gerber S, Charif M, Chevrollier A, et al. Mutations in DNM1L, as in OPA1, result in dominant optic atrophy despite opposite effects on mitochondrial fusion and fission. Brain 2017;140:2586–2596.
23. Charif M, Roubertie A, Salime S, et al. A novel mutation of AFG3L2 might cause dominant optic atrophy in patients with mild intellectual disability. Front Genet 2015;6:311.
24. Colavito D, Maritan V, Suppiej A, et al. Non-syndromic isolated dominant optic atrophy caused by the p.R468C mutation in the AFG3 like matrix AAA peptidase subunit 2 gene. Biomed Rep 2017;7: 451–454.
25. Magri S, Fracasso V, Plumari M, et al. Concurrent AFG3L2 and SPG7 mutations associated with syndromic parkinsonism and optic atrophy with aberrant OPA1 processing and mitochondrial network fragmentation. Hum Mutat 2018;39:2060–2071.
26. Esser K, Tursun B, Ingenhoven M, et al. A novel two-step mechanism for removal of a mitochondrial signal sequence involves the mAAA complex and the putative rhomboid protease Pcp1. J Mol Biol 2002; 323:835–843.
27. Nolden M, Ehses S, Koppen M, et al. The m-AAA protease defective in hereditary spastic paraplegia controls ribosome assembly in mitochondria. Cell 2005;123:277–289.
28. Koppen M, Langer T. Protein degradation within mitochondria: versatile activities of AAA proteases and other peptidases. Crit Rev Biochem Mol Biol 2007;42:221–242.
29. Di Bella D, Lazzaro F, Brusco A, et al. Mutations in the mitochondrial protease gene AFG3L2 cause dominant hereditary ataxia SCA28. Nat Genet 2010;42:313–321.
30. Pierson TM, Adams D, Bonn F, et al. Whole-exome sequencing identifies homozygous AFG3L2 mutations in a spastic ataxia-neuropathy syndrome linked to mitochondrial m-AAA proteases. PLoS Genet 2011;7:e1002325.
31. Del Dotto V, Fogazza M, Musiani F, et al. Deciphering OPA1 mutations pathogenicity by combined analysis of human, mouse and yeast cell models. Biochim Biophys Acta Mol Basis Dis 2018;1864: 3496–3514.
32. Nasca A, Nardecchia F, Commone A, et al. Clinical and biochemical features in a patient with mitochondrial fission factor gene alteration. Front Genet 2018;9:625 Available at: https://www.frontiersin.org/articles/10.3389/fgene.2018.00625/full. Accessed September 20, 2019.
33. Invernizzi F, Ardissone A, Lamantea E, et al. Cavitating leukoencephalopathy with multiple mitochondrial dysfunction syndrome and NFU1 mutations. Front Genet 2014;5:412.
34. Tatsuta T, Augustin S, Nolden M, et al. M-AAA protease-driven membrane dislocation allows intramembrane cleavage by rhomboid in mitochondria. EMBO J 2007;26:325–335.
35. Bonn F, Tatsuta T, Petrungaro C, et al. Presequence-dependent folding ensures MrpL32 processing by the m-AAA protease in mitochondria. EMBO J 2011;30:2545–2556.
36. Song Z, Chen H, Fiket M, et al. OPA1 processing controls mitochondrial fusion and is regulated by mRNA splicing, membrane potential, and Yme1L. J Cell Biol 2007;178:749–755.
37. Klebe S, Depienne C, Gerber S, et al. Spastic paraplegia gene 7 in patients with spasticity and/or optic neuropathy. Brain 2012;135: 2980–2993.
38. Hartmann B, Wai T, Hu H, et al. Homozygous YME1L1 mutation causes mitochondriopathy with optic atrophy and mitochondrial network fragmentation. Elife 2016;5:e16078.
39. Patron M, Sprenger H-G, Langer T. m-AAA proteases, mitochondrial calcium homeostasis and neurodegeneration. Cell Res 2018;28: 296–306.
40. Richter U, Lahtinen T, Marttinen P, et al. Quality control of mitochondrial protein synthesis is required for membrane integrity and cell fitness. J Cell Biol 2015;211:373–389.
41. Almajan ER, Richter R, Paeger L, et al. AFG3L2 supports mitochondrial protein synthesis and Purkinje cell survival. J Clin Invest 2012; 122:4048–4058.
42. Maltecca F, De Stefani D, Cassina L, et al. Respiratory dysfunction by AFG3L2 deficiency causes decreased mitochondrial calcium uptake via organellar network fragmentation. Hum Mol Genet 2012;21: 3858–3870.

43. Ferreirinha F, Quattrini A, Pirozzi M, et al. Axonal degeneration in paraplegin-deficient mice is associated with abnormal mitochondria and impairment of axonal transport. J Clin Invest 2004;113:231–242.

44. Pfeffer G, Gorman GS, Griffin H, et al. Mutations in the SPG7 gene cause chronic progressive external ophthalmoplegia through disordered mitochondrial DNA maintenance. Brain 2014;137:1323–1336.

45. Yu-Wai-Man P, Votruba M, Burté F, et al. A neurodegenerative perspective on mitochondrial optic neuropathies. Acta Neuropathol 2016;132:789–806.

46. Burté F, Carelli V, Chinnery PF, Yu-Wai-Man P. Disturbed mitochondrial dynamics and neurodegenerative disorders. Nat Rev Neurol 2015;11:11–24.

47. Puchades C, Ding B, Song A, et al. Unique structural features of the mitochondrial AAA+ protease AFG3L2 reveal the molecular basis for activity in health and disease. Mol Cell 2019;75:1073–1085.e6.

48. Koppen M, Bonn F, Ehses S, Langer T. Autocatalytic processing of m-AAA protease subunits in mitochondria. Mol Biol Cell 2009;20:4216–4224.

49. Mancini C, Hoxha E, Iommarini L, et al. Mice harbouring a SCA28 patient mutation in AFG3L2 develop late-onset ataxia associated with enhanced mitochondrial proteotoxicity. Neurobiol Dis 2019;124:14–28.

50. Carelli V, Sabatelli M, Carrozzo R, et al. "Behr syndrome" with OPA1 compound heterozygote mutations. Brain 2015;138:e321.